

Supporting Information

Zinc-Selenium Synergistic Nanoplatfom for Augmented Cancer Immunotherapy via Trace elements-mediated Immunomodulation

Hang Liu^{ab}, Mingjing Cao^{*b}, Weixian Zhou^{bc}, Lu Li^{bc} and Chunying Chen^{*bc}

^a School of Biomedical Sciences and Engineering, South China University of Technology, Guangzhou International Campus, Guangzhou 511442, China

^b CAS Key Laboratory for Biomedical Effects of Nanomedicines and Nanosafety & CAS Center for Excellence in Nanoscience, National Center for Nanoscience and Technology of China, Beijing 100190, China

^c University of Chinese Academy of Sciences, Beijing 100049, China

* Address correspondence to caomj@nanoctr.cn, chenchy@nanoctr.cn

Materials and methods

Materials and instruments

All chemical reagents and raw materials were purchased from chemical suppliers and used as received without purification. Sodium selenite is purchased from Merck, Zinc Acetate, Sodium Sulfate from Macklin, BSA from Yihong Guangjie Biotechnology, NHS-Cy5 and LysoTracker Green from Invitrogen. APC anti-mouse CD3, Ghost Dye™ Violet 510, FITC anti-mouse CD11c, PE anti-mouse CD8a, PE anti-mouse CD80 antibodies were purchased from TonBo, PerCP/Cyanine5.5 anti-mouse CD86, APC anti-mouse MHCII, APC-Cy7 anti-mouse CD45, PC5.5 anti-mouse CD4, APC anti-mouse IFN- γ antibodies were purchased from BioLegend. SelK polyclonal antibody was purchased from Proteintech, GPX4 antibody from Affinity, GAPDH antibody, p-TBK1 antibody, and p-IRF3 antibody from Abcam. The ELISA kit was purchased from MEIMIAN.

Synthesis of ZSB NCs, ZB NPs and SeB NPs

40 mg BSA dissolved in 6 mL water, blending with zinc acetate dihydrate (150 mM) and stirring rigorously for 5 minutes. Followed by adding sodium selenite (75 mM) and sodium sulfide (466 mM), the mixture solution kept reacting for 4 hours at room temperature. Finally, the solution was dialyzed (MWCO: 10000) to remove the unreacted reagents, then ZSB NCs was obtained. To synthesize ZB NPs and SeB NPs, previous steps are repeated, but the addition of sodium selenite and zinc acetate dihydrate was removed, respectively.

To covalently label ZSB NCs with Cy5 fluorescence dyes, 1 mL of ZSB NCs suspension (2 mg/mL) was mixed with 100 μ L of NaHCO₃ solution (1 M) to adjust the pH to 8.5–9.0. Subsequently, 20 μ L of NHS-Cy5 solution (10 mg/mL) was added, and the reaction was allowed to proceed for 2 h at room temperature with stirring at 400 rpm and protection from light. The resulting mixture was purified using a 10 kDa centrifugal filter to remove excess NHS-Cy5 by centrifugation at 7500 rpm for 15 min, and repeated until the filtrate became colorless. The colloidal stability was tested with the following steps: The purified ZSB NCs-Cy5 was uniformly dispersed in PBS buffer supplemented with FBS and stored at room temperature in the dark. Samples were subjected to ultrafiltration at 0, 1, and 3 days. Each time, the filtrate was collected, and the retentate was

redispersed in 2 mL of fresh PBS buffer supplemented with FBS. Fluorescence spectra of both the ZSB NCs-Cy5 conjugate and the corresponding filtrates at different time points were recorded for analysis.

Characterization of ZSB NCs

The morphology of nanoclusters was observed using a transmission electron microscope (Tecnaï G2 20 S-TWIN) and a cold field emission scanning electron microscope (Hitachi S4800). The elemental mapping of nanoclusters was observed using a field emission transmission electron microscope (Tecnaï G2 F20 U-TWIN). The zeta potential and dynamic light scattering (DLS) were measured using a Malvern instrument Zetasizer Nano system. TEM images were analyzed for particle size using ImageJ, and X-ray photoelectron spectroscopy (XPS) spectra were recorded using an ESCALAB250Xi X-ray photoelectron spectrometer. XANES (beamline 1W1B of the Beijing Synchrotron Radiation Facility (BSRF)) was applied to determine chemical forms of ZSB NCs and the biotransformation of Zn and Se in DCs. The stability of ZSB NCs was evaluated in PBS and PBS buffer supplemented with FBS to simulate the extracellular environment. The hydrodynamic diameter and zeta potential of the samples were measured by dynamic light scattering (DLS) at 1, 3, 5, 7, 14, and 30 days.

Cell culture

DC2.4 cells were cultured in RPMI 1640 medium, with 10% fetal bovine serum (FBS), 100 U/mL sodium penicillin G, and 100 mg/mL streptomycin sulfate, 0.4% β -mercaptoethanol, and 1% HEPES. 4T1 cells were cultured in RPMI 1640 medium with 10% FBS and 1% penicillin-streptomycin (PS), while HSF cells were cultured in DMEM medium with 10% FBS and 1% PS. All cells were incubated under 5% CO₂ at 37 \pm 1 $^{\circ}$ C.

Bone marrow-derived dendritic cells (BMDCs) were obtained from the tibia and femur of 6-week-old female C57BL/6 mice and filtered through a 70 μ m sieve. Then, the cells were cultured in RPMI 1640 medium supplemented with 10% FBS, 1% PS, 20 ng/ml GM-CSF, 2 mM L-glutamine, and 50 μ M β -mercaptoethanol after centrifugation and remove the red blood cells.

Animal experimentation

All experiments in this study were performed in compliance with the relevant laws and guidelines of the Institutional Animal Care and Use Committee of the National Center for Nanoscience and Technology, China (Ethical approval number: NCNST21-202503-0014) and also the Institutional Animal Care and Use Committee of the National Center for Nanoscience and Technology have approved the experiments. Informed consent was obtained for any experimentation with animal subjects. SPF grade BALB/c mice (4 weeks old, female) were purchased from Home SPF (Beijing) Biotechnology Co., Ltd. To establish a tumor bearing model 100 μ L 4T1 cells PBS suspension (5.0×10^7 /mL cells) was subcutaneously injected into the mammary gland in mice for the tumor animal model.

***In vivo* and *in vitro* fluorescence imaging**

After subcutaneous injection of ZSB NCs-Cy5 and free NHS-Cy5 into tumor bearing mice, *in vivo* imaging and biological distribution were investigated using an imaging system (IVIS Lumina) at different time points.

After co-incubating ZSB NCs-Cy5 with DC2.4 for 2 hours, lysosomes and nucleus were stained with LysoTracker green and Hoechst respectively, then observed using Leica white light laser confocal imaging system (Stellaris 8).

Biodistribution quantitation of ZSB NCs and SR-XRF imaging of lymph nodes

After subcutaneous injection of ZSB NCs into tumor bearing mice, the main organs, tumors, and lymph nodes of the mice were collected at different time points (n=4). A portion of the tissue was digested and the distribution of Zn and Se in the body was quantified by ICP-MS. The other portion was embedded with OCT and frozen sectioned, and SR-XRF imaging was performed using the beam line 4W1B of the Beijing Synchrotron Radiation Facility (BSRF) in China.

Activation of Dendritic Cells *In Vitro* measured by flow cytometry and Western blotting

DC2.4 cells were seeded in 6-well plates and cultured overnight. They were then treated for 24 hours with ZSB NCs at concentrations of 0, 0.1, 0.5, and 1 μ g/mL, as well as with ZB NPs, SeB NPs, mixture of ZB NPs and SeB NPs (ZB NPs+ SeB NPs), and ZSB NCs, all at equivalent elemental doses. After treatment, the cells were harvested and divided into two portions for

subsequent analysis. One portion was centrifuged and resuspended in PBS buffer supplemented with FBS, followed by staining in the dark at 4 °C for 20 minutes with the following antibodies: Ghost Dye™ Violet 510 viability dye, PE anti-mouse CD80, PerCP/Cyanine5.5 anti-mouse CD86, and APC anti-mouse MHCII. After staining, the cells were washed and subjected to flow cytometry analysis. The others were lysed to extract total proteins. Western blotting was performed to evaluate the expression levels of IRF3, TBK1, phosphorylated IRF3 (p-IRF3), phosphorylated TBK1 (p-TBK1), GPX4, and SelK.

***In vivo* antitumor effects**

To evaluate the immunomodulatory anti-tumor effect of ZSB NCs, tumor bearing mice were randomly divided into four groups (n=5) on day 3 post-operation: PBS group, ZSB NCs group, ZnS/BSA group, and Se/BSA group. The nanomedicine was injected by subcutaneous every 3 days for three times, and each mouse was injected with 100 µL (400 µg/mL). The tumor volume and body weight of mice were recorded every two days. The mice were euthanized when average tumor volume of PBS group mice reaches 1500 mm³. Along with tumor tissue, the main organs of mice (heart, liver, spleen, lungs, kidneys) were also harvested and subjected to H&E staining.

Detection of lymphocytes in the tumor and lymph node

Tumor tissues and lymph nodes were harvested. A portion of the tumor was fixed with 4% paraformaldehyde for immunohistochemistry to analyze the infiltration of CD4⁺ T cells and CD8⁺ T cells in the tumor tissue microenvironment. The other part was detected with flow cytometry to analyze the infiltration of T cells in the tumor tissue microenvironment. Tumor tissue and lymph nodes were mechanically divided into small pieces, and digested with collagenase to form the single-cell suspension. Single-cell suspensions were then filtered through a 70 µm sterile mesh and resuspended with sterile PBS after centrifugation at 200 g for 5 minutes. Followed by the incubation with different flow cytometry antibodies such as APC anti-mouse CD3 and APC-Cy7 anti-mouse CD45 antibodies in the dark for 30 minutes, the stained the single-cell suspensions were washed with PBS before the flow cytometry assay.

ELISA assay

Blood was collected from the eyes of the mice, and the serum was collected after centrifugation.

The levels of CXCL10, IFN- γ , TNF- α and IL-1 β in blood serum were detected using ELISA kits, according to the instructions from the manufacturer.

Safety evaluation of the ZSB NCs

The in vitro biocompatibility was first assessed by MTT assay. Specifically, DC2.4 cells were seeded in 96-well plates overnight and then incubated for 24 hours with ZB NPs, SeB NPs, ZB NPs+ SeB NPs, or ZSB NCs (all at elemental doses equivalent to that of ZSB NCs). Furthermore, the cytotoxicity of ZSB NCs at varying concentrations was evaluated in BMDC, HSF, and HaCaT cell lines. After seeding the cells in 96-well plates and allowing them to adhere overnight, they were treated with different concentrations of ZSB NCs for 24 hours. Subsequently, cell viability was determined using the MTT assay.

The body weight and tumor size of the mice were recorded every two days, and the tumor bearing mice were euthanized at day 24. The main tumor tissues and organs, including the heart, liver, spleen, lungs, and kidneys were harvested. They were subsequently fixed with 4% paraformaldehyde, for H&E staining and analysis.

Statistical analysis

All data were presented as mean \pm standard deviation (SD). Differences between experimental groups were analyzed using one-way ANOVA with Tukey's multiple-comparisons test conducted using GraphPad software (Inc., LaJolla, CA, USA). Significance was determined by P-values, where * $P < 0.05$, ** $P < 0.01$, *** $P < 0.001$, and **** $P < 0.0001$.

Supporting Figures

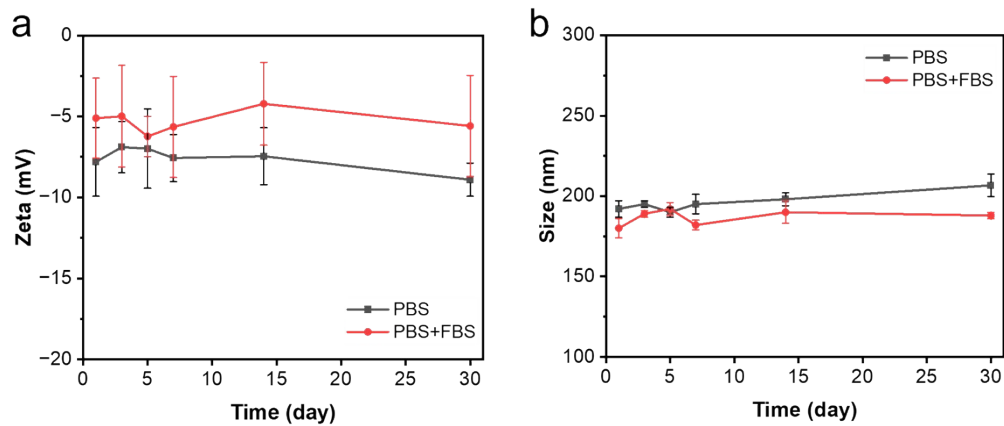


Fig. S1. Measurement of zeta potential (a) and hydrodynamic diameter (b) of ZSB NCs incubated in PBS and PBS buffer supplemented with FBS (pH 7.4) during 30 day-time period.

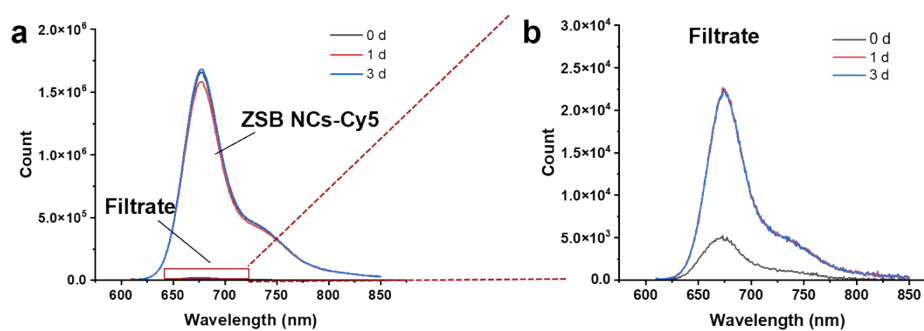


Fig. S2. The fluorescence spectrum of ZSB NCs-Cy5 (a) and filtrate (b).

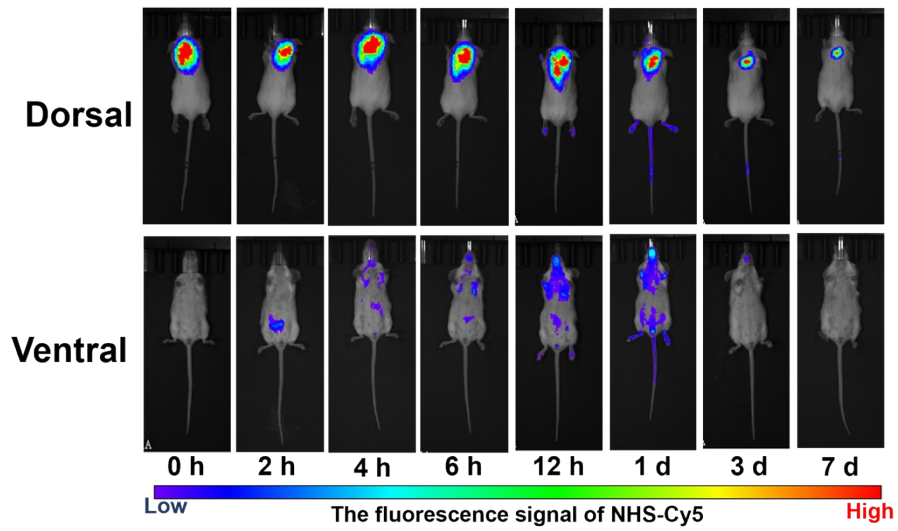


Fig. S3. The in vivo fluorescent imaging at different time points after subcutaneous injection with free NHS-Cy5.

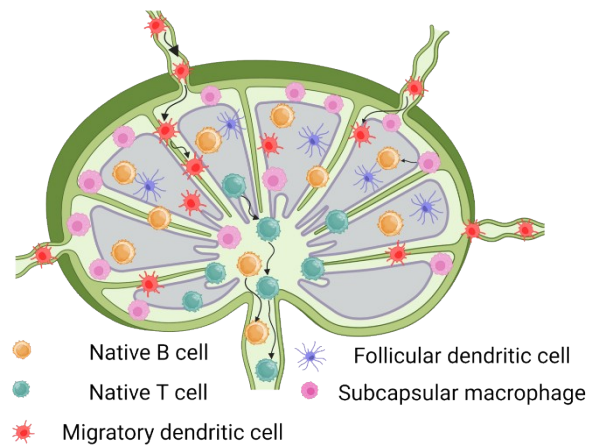


Fig. S4. Schematic illustration of immune cell subtypes in a lymph node cross-section.

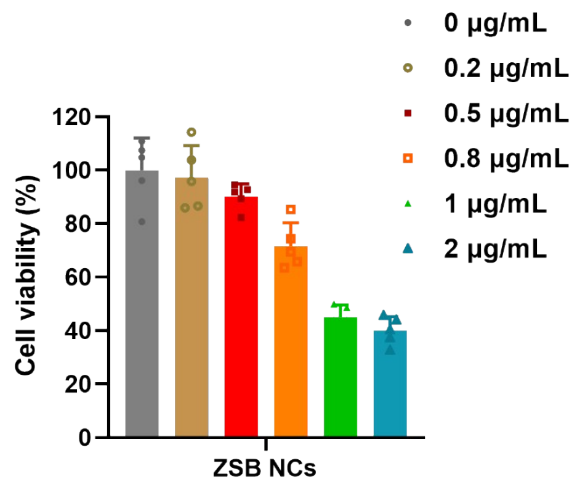


Fig. S5. Cytotoxicity of ZSB NCs to BMDC cells. Data are presented as the mean \pm SD.

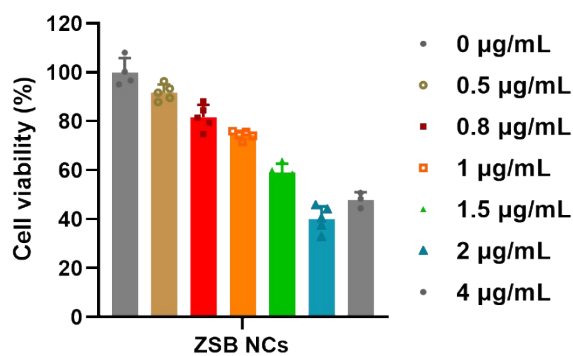


Fig. S6. Cytotoxicity of ZSB NCs to DC 2.4 cells. Data are presented as the mean \pm SD.

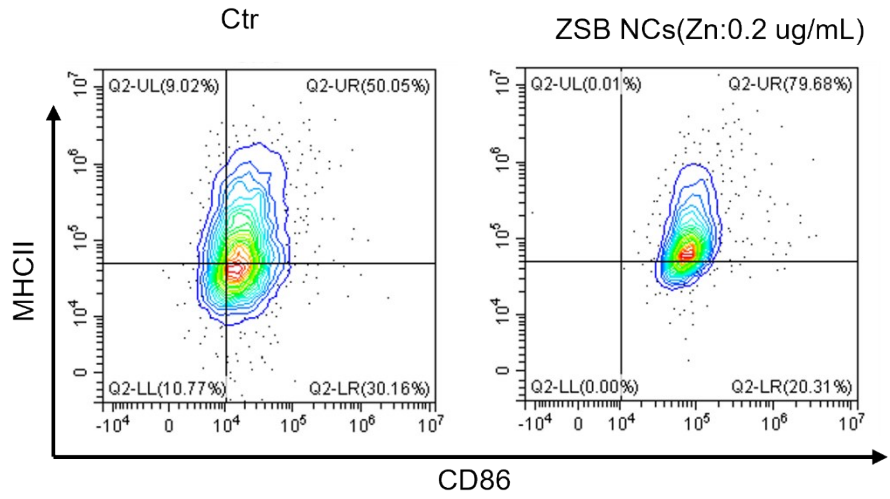


Fig. S7. Flow cytometry analysis of the percentages of CD86⁺MHCII⁺ cells in BMDC.

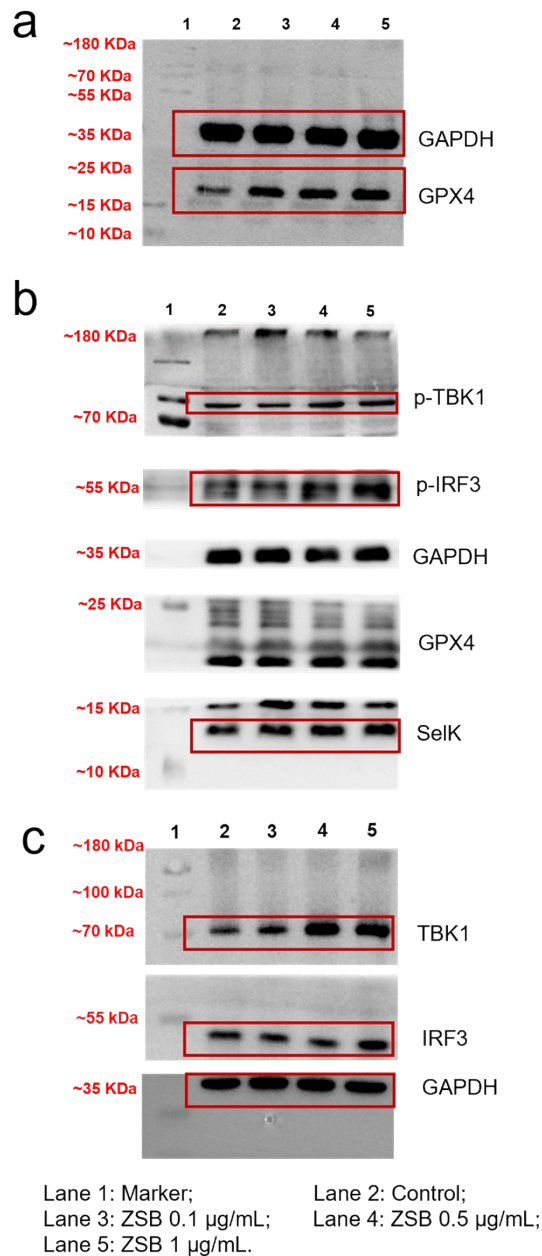


Fig. S8. Raw images of TBK1, IRF3, p-TBK1, p-IRF3, GAPDH, GPX4, and SelK in BMDC by Western blot assay. Following transfer from the gel to the membrane, the membrane was sectioned into five strips based on the molecular weights of the target proteins. These strips were then blocked for 1 hour at room temperature, washed five times with TBST (Tris-buffered saline containing 0.1% Tween 20), and subsequently incubated overnight at 4°C with their respective primary antibodies. This approach was adopted for the following reasons: 1) To minimize non-specific binding of antibodies and reduce the background signal; 2) To allow each individual membrane strip to be incubated with primary and secondary antibodies under

optimal conditions (e.g., specific incubation time, dilution buffer); 3) To enable the simultaneous detection of both internal reference proteins and interested proteins in one blot; 4) To reduce antibody consumption and lower costs. After three additional TBST washes, the strips were incubated with horseradish peroxidase-conjugated immunoglobulin G (ZSGB-BIO) for 1 hour at 4°C. Following final washes, protein bands were visualized using the Super ECL Detection Reagent-ECL Chemiluminescence Ultra-High Sensitivity Color Development Kit (Yeasen), and images were captured using the Luminescence Imaging System (ChemiScope 6100). We acquired the image of all strips simultaneously by assembling the segmented strips, showing the GAPDH and GPX4 bands (a). Images of p-TBK1, p-IRF3, and SelK bands (b) and TBK1, IRF3 bands (c) in another membrane were individually acquired since simultaneous imaging resulted in the non-detection of proteins with low expression levels.

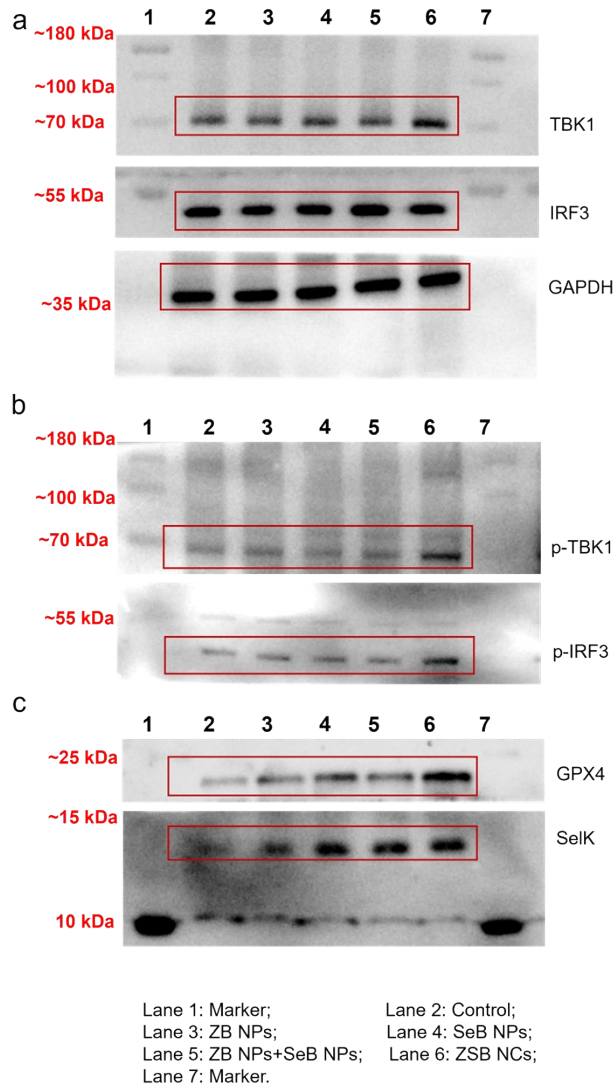


Fig. S9. Raw images of TBK1, IRF3, p-TBK1, p-IRF3, GAPDH, GPX4, and SelK in BMDC by Western blot assay. Same procedure used in Fig. S8 was adopted with brief revision: the membranes containing the protein bands for p-IRF3 and p-TBK1 were stripped with stripping buffer for 30 minutes after image capture. They were then re-blocked and subsequently incubated with primary antibodies against IRF3 and TBK1, followed by the standard subsequent processing and imaging. (a) TBK1, IRF3 and GAPDH bands; (b) p-TBK1 and p-IRF3 bands; (c) GPX4 and SelK bands.

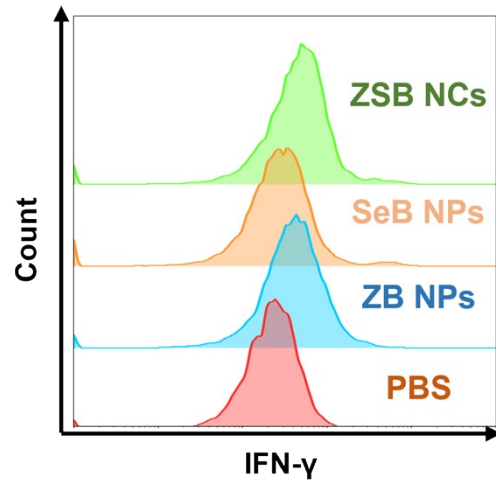


Fig. S10. Flow cytometry analysis of the percentages of IFN- γ in tumor (n=3).

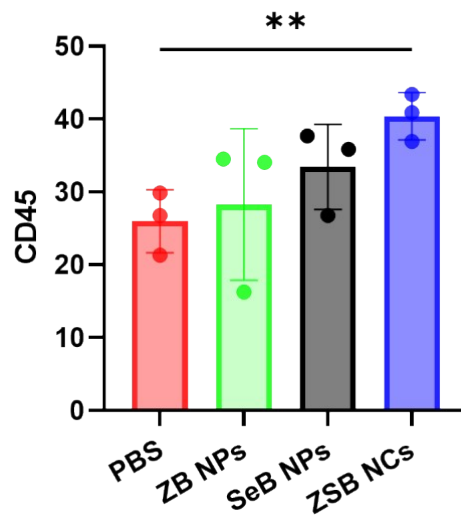


Fig. S11. Flow cytometry analysis of the percentages of CD45⁺ lymphocytes in tumor. Data are presented as the mean \pm SD.

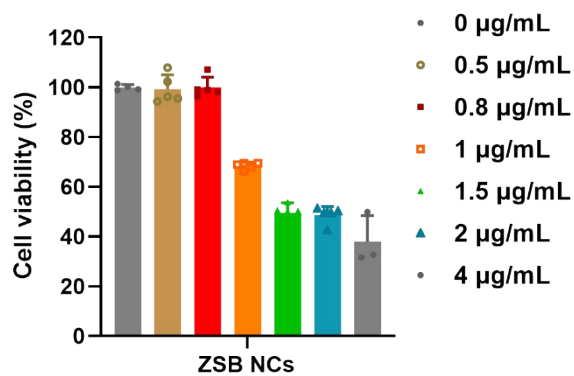


Fig. S12. Cytotoxicity of ZSB NCs to HSF cells. Data are presented as the mean \pm SD.

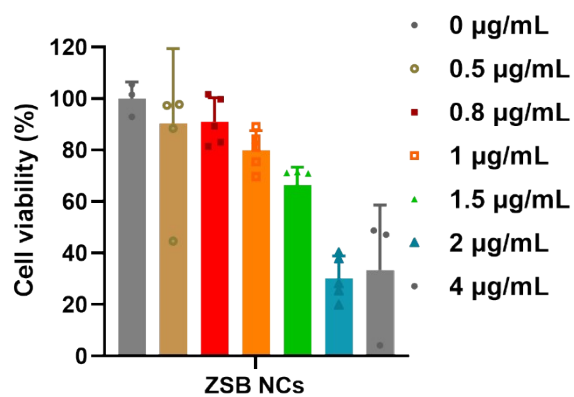


Fig. S13. Cytotoxicity of ZSB NCs to 4T1 cells. Data are presented as the mean \pm SD.

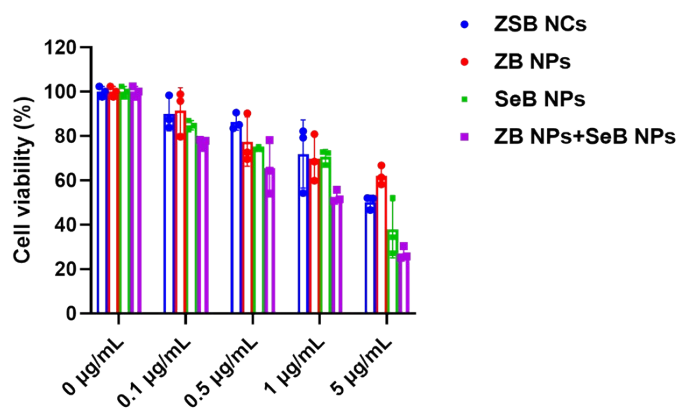


Fig. S14. Cytotoxicity of different treatment to DC2.4 cells. Data are presented as the mean \pm SD

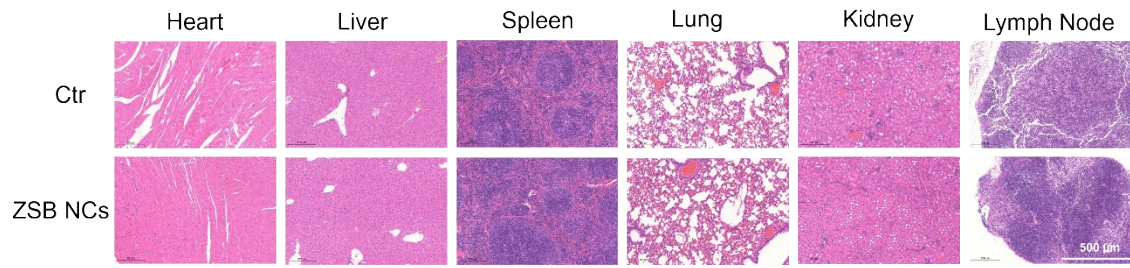


Fig. S15. Hematoxylin and eosin (H&E) staining images of the heart, liver, spleen, lung, kidney and lymph node tissues of mice treated with ZSB NCs. Scale bar: 500 μm .